

UNLIMITED  
UNCLASSIFIED

Canada

(4)

AD-A211 654

# ANALYSIS OF EXPERIMENTAL DATA FOR CAST 10-2/DOA 2 SUPERCRITICAL AIRFOIL AT LOW REYNOLDS NUMBERS AND APPLICATION TO HIGH REYNOLDS NUMBER FLOW

by

Y.Y. Chan

National Aeronautical Establishment

OTTAWA  
JANUARY 1989

AERONAUTICAL NOTE  
NAE-AN-80  
NRC NO. 80268



National Research  
Council Canada

Conseil national  
de recherches Canada

## NATIONAL AERONAUTICAL ESTABLISHMENT

### SCIENTIFIC AND TECHNICAL PUBLICATIONS

#### AERONAUTICAL REPORTS

**Aeronautical Reports (LR):** Scientific and technical information pertaining to aeronautics considered important, complete, and a lasting contribution to existing knowledge.

**Mechanical Engineering Reports (MS):** Scientific and technical information pertaining to investigations outside aeronautics considered important, complete, and a lasting contribution to existing knowledge.

**AERONAUTICAL NOTES (AN):** Information less broad in scope but nevertheless of importance as a contribution to existing knowledge.

**LABORATORY TECHNICAL REPORTS (LTR):** Information receiving limited distribution because of preliminary data, security classification, proprietary, or other reasons.

Details on the availability of these publications may be obtained from:

Graphics Section,  
National Research Council Canada,  
National Aeronautical Establishment,  
Bldg. M-16, Room 204,  
Montreal Road,  
Ottawa, Ontario  
K1A 0R6

## ÉTABLISSEMENT NATIONAL D'AÉRONAUTIQUE PUBLICATIONS SCIENTIFIQUES ET TECHNIQUES

#### RAPPORTS D'AÉRONAUTIQUE

**Rapports d'aéronautique (LR):** Informations scientifiques et techniques touchant l'aéronautique jugées importantes, complètes et durables en termes de contribution aux connaissances actuelles.

**Rapports de génie mécanique (MS):** Informations scientifiques et techniques sur la recherche externe à l'aéronautique jugées importantes, complètes et durables en termes de contribution aux connaissances actuelles.

**CAHIERS D'AÉRONAUTIQUE (AN):** Informations de moindre portée mais importantes en termes d'accroissement des connaissances.

**RAPPORTS TECHNIQUES DE LABORATOIRE (LTR):** Informations peu disséminées pour des raisons d'usage secret, de droit de propriété ou autres ou parce qu'elles constituent des données préliminaires.

Les publications ci-dessus peuvent être obtenues à l'adresse suivante:

Section des graphiques,  
Conseil national de recherches Canada,  
Établissement national d'aéronautique,  
Im. M-16, pièce 204,  
Chemin de Montréal,  
Ottawa (Ontario)  
K1A 0R6

UNLIMITED  
UNCLASSIFIED

**ANALYSIS OF EXPERIMENTAL DATA FOR  
CAST 10-2/DOA 2 SUPERCRITICAL AIRFOIL AT  
LOW REYNOLDS NUMBERS AND APPLICATION  
TO HIGH REYNOLDS NUMBER FLOW**

**ANALYSE DES DONNÉES EXPÉRIMENTALES DE L'AILE  
SUPERCRITIQUE CAST 10-2/DOA 2 AUX FAIBLES NOMBRES  
DE REYNOLDS ET APPLICATION DES RÉSULTATS AUX  
SIMULATIONS D'ÉCOULEMENT D'AIR À DES NOMBRES  
DE REYNOLDS ÉLEVÉS**

**by/par**

**Y.Y. Chan**

**National Aeronautical Establishment**

**OTTAWA  
JANUARY 1989**

**DTIC  
ELECTE  
AUG 22 1989  
S B D**

**AERONAUTICAL NOTE  
NAE-AN-60  
NRC NO. 30268**

**Y.Y. Chan, Head/Chef  
High Speed Aerodynamics Laboratory/  
Laboratoire d'aérodynamique à hautes vitesses**

**G.F. Marsters  
Director/directeur**

## ABSTRACT

The experimental investigation of CAST 10-2/DOA 2 supercritical airfoil previously conducted in the NAE Two-Dimensional Test Facility has been extended to low Reynolds number range at the design Mach number 0.765. The results indicate that with forward transition fixing, the data trend at low Reynolds number is different from that at high Reynolds number with the former more sensitive to the Reynolds number variation. The dividing Reynolds number for these two regions is about 10 million. With aft fixing, the low Reynolds number data approach those at higher Reynolds numbers for cruise conditions. However, at high lift conditions the thin boundary layer delays separation and higher maximum lift is obtained. The characteristics of the Reynolds number dependency obtained from the analysis substantiate the principle of the simulation/extrapolation methodology for data obtained from low Reynolds number to flight Reynolds number as proposed by the AGARD/Fluid Dynamics Panel.

## RÉSUMÉ

L'expérience sur l'aile supercritique CAST 10-2/DOA 2 qui avait été menée dans la veine d'essai bidimensionnel de l'ENA s'est poursuivie à des nombres de Reynolds plus faibles et au nombre de Mach 0,765. Lorsque la transition de la couche limite est fixée sur la partie avant de l'aile, les résultats montrent que la tendance des données aux nombres de Reynolds faibles est différente de celle des nombres de Reynolds élevés, la première étant plus sensible aux variations du nombre de Reynolds. Le nombre de Reynolds qui divise ces deux régions se situe à environ 10 millions. Si la transition est fixée sur la partie arrière de l'aile, les données pour les nombres de Reynolds faibles s'approchent de celles obtenues aux nombres de Reynolds élevés dans les conditions de vol en croisière. Lorsque la portance est élevée cependant, la mince couche limite retarde le décollement et on obtient ainsi une portance maximale plus grande. Les caractéristiques de la dépendance des nombres de Reynolds qui ont été remarquées pendant l'analyse confirment le principe de la méthode de simulation et d'extrapolation des données proposée par le comité sur la dynamique des fluides de l'AGARD. Les données ont été obtenues à partir de nombres de Reynolds faibles allant jusqu'à des nombres de Reynolds couramment rencontrés en vol.

(iii)

Accession For	
NTIS GRA&I	<input checked="" type="checkbox"/>
DTIG TAB	<input type="checkbox"/>
Unannounced	<input type="checkbox"/>
Justification	
By	
Distribution/	
Availability Codes	
Dist	Avail and/or Special
A-1	

## Table of Contents

	<b>Page</b>
Summary	(iii)
List of Figures	(v)
Symbols	(vii)
1. Introduction	1
2. Reynolds Number Effects	3
2.1 Lift, Pitching Moment and Drag	5
2.2 Shock Location and Shock Mach Number	7
2.3 Trailing Edge Pressure	10
2.4 General Characteristics of Low Reynolds Number Flow	11
3. Simulation and Extrapolation	11
4. Conclusion	15
References	17

## List of Figures

### Figure

- 1 Section profile of CAST 10-2/DOA 2 airfoil
- 2 Estimations of natural transition locations at the upper surface of the airfoil,  $M_{\infty} = 0.765$
- 3a Lift versus angles of attack at various Reynolds numbers with forward and aft transition fixings,  $M_{\infty} = 0.765$
- 3b Reynolds number dependence of lift at an angle of attack  $\alpha = 1.35$  degrees,  $M_{\infty} = 0.765$
- 4a Pitching moment versus lift at various Reynolds numbers with forward and aft transition fixings,  $M_{\infty} = 0.765$
- 4b Reynolds number dependence of pitching moment at constant lift  $C_{Lp} = 0.65$ ,  $M_{\infty} = 0.765$
- 5a Drag versus lift at various Reynolds numbers with forward and aft transition fixings,  $M_{\infty} = 0.75$
- 5b Reynolds number dependence of drat at constant lift  $C_{Lp} = 0.65$ ,  $M_{\infty} = 0.765$
- 6a Shock location versus lift at various Reynolds number with forward and aft transition fixings,  $M_{\infty} = 0.765$
- 6b Reynolds number dependence of shock location at constant lift  $C_{Lp} = 0.65$ ,  $M_{\infty} = 0.765$
- 7a Shock Mach number versus lift at various Reynolds number with forward and aft transition fixings,  $M_{\infty} = 0.765$
- 7b Reynolds number dependence of shock Mach number at constant lift  $C_{Lp} = 0.65$ ,  $M_{\infty} = 0.765$

Figure

8a Trailing edge pressure versus lift at various Reynolds number with forward and aft transition fixings,  $M_{\infty} = 0.765$

8b Reynolds number dependence of trailing edge pressure at constant lift  $C_{Lp} = 0.65, M_{\infty} = 0.765$

9 Computational results for the simulation criterion in comparison with experimental data,  $C_{Lp} = 0.65, M_{\infty} = 0.765$ .

### List of Symbols

$c$	chord length
$C_{D_W}$	drag coefficient, wake integration
$C_{L_P}$	lift coefficient, pressure integration
$C_m$	pitching moment coefficient, quarter chord
$C_{p_{T.E.}}$	pressure coefficient, trailing edge
$M_\infty$	free stream Mach number
$M_s$	shock Mach number
$Re_c$	free stream Reynolds number based on chord length
$x, y$	Cartesian coordinates, $x$ in chordwise direction
$x_s$	shock position on model
$x_T$	transition location
$\alpha$	angle of attack

## 1. Introduction

Extrapolating aerodynamic characteristics of an airfoil or a wing from model testing in a wind tunnel at low Reynolds numbers to flight Reynolds number, usually having a much higher value than that of the model testing, is always difficult because of the highly nonlinear behaviour of the boundary layer. The problem is exaggerated at transonic speeds as the inviscid flow is extremely sensitive to the effective change of the shape of the profile due to the boundary layer displacement. The presence of shock waves at the airfoil surface as the local flow becomes supercritical further increases the complexity of the viscous-inviscid interaction. Although the subject has been extensively studied, the overall picture has remained rather muddled and this led to the establishment of a Working Group (09) by the AGARD Fluid Dynamics Panel to provide an overall summary of the state of the art and to recommend the proper procedure for wind tunnel simulation. <sup>(1)</sup>

The simulation methodology proposed by the work group consists of two approaches: (i) Reynolds number sweeps with transition fixed near the leading edge close to where it may occur at the flight Reynolds number; (ii) with manipulation of the boundary layer by aft-transition fixing technique to produce a viscous flow behaviour near the trailing edge close to that at the flight Reynolds number. The first approach requires a variable density wind tunnel with wide Reynolds number range and the second approach is suitable for a constant density tunnel with limited Reynolds number capability.

In the last two years, a series of tests has been performed in the NAE High Speed Aerodynamics Laboratory on a supercritical airfoil with the CAST 10-2/DOA 2 profile at high Reynolds numbers. The investigation was a part of a NAE/NRC-NASA Langley Cooperative Program on Two-Dimensional Wind tunnel Wall Interference Research. The program concentrated mainly on data at high Reynolds numbers from 10 to 30 million, with tests carried out in both laboratories. The results have been presented in two reports<sup>(2,3)</sup> and the data analysed for effects of Reynolds and Mach numbers.<sup>(4)</sup> This investigation shows that at the high Reynolds number range, the aerodynamic characteristics of the airfoil depends only weakly on the Reynolds number variation. Extrapolation of the airfoil performance to a higher Reynolds number can readily be carried out.

At low Reynolds number, the characteristics of the airfoil may not follow the trend of high Reynolds number. The effect on lift coefficient at a fixed angle of attack, has been demonstrated by Stanewsky et al, for Reynolds numbers 2 to 30 million<sup>(5)</sup>. Extrapolation from low Reynolds number data becomes less straightforward. To provide a more detailed view of Reynolds number dependency as well as the effects of transition location, especially in the low Reynolds number range, a test program has been carried out to extend the range of the existing data set at the low Reynolds number end from 10 to 4.2 million, the lower limit of the tunnel performance. The test was conducted at a Mach number of 0.765, the design value of the airfoil. With the high Reynolds number data, the extended data bank for forward transition fixing now covers a wide range of Reynolds number from 4.2 to 30 million. With aft-fixings at 30 and 45 percent chord respectively, data were obtained for Reynolds numbers 4.2 to 8 million. The test program and the results were reported in Reference 6.

The data bank covering such a wide range of Reynolds number allows us to study the viscous effect in accordance with the first procedure recommended by the AGARD methodology, Reynolds number sweep. It is important to delineate the behaviours of the aerodynamic parameters at low Reynolds numbers as they may be quite different from those at high Reynolds numbers. These behaviours directly determine the strategy of extrapolation in the methodology.<sup>(1)</sup> The data at low Reynold's numbers with aft-fixing will be examined in the light of the second procedure on simulation, boundary layer manipulation. The Reynolds number range at which the flow can be simulated will be determined.

In what follows, the low Reynolds number characteristics of the airfoil will be first presented. The two aspects of simulation/extrapolation will then be examined in some detail with data at both low and high Reynolds numbers.

## 2. Reynolds Number Effects

At transonic speeds the flow past an airfoil is extremely sensitive to the slightest variation of the airfoil contour. As the boundary layer develops over the airfoil, the displacement thickness of the boundary layer effectively changes the airfoil profile and the pressure distribution. Thus the performance of the airfoil depends on the boundary layer development and hence the free stream Reynolds number. At high Reynolds numbers this dependency is weak. The effect shows mainly in changes of the boundary layer properties with Reynolds number such as displacement thickness and skin friction. Even with free transition, the effect is not strong as the forward shift of the transition position compensates for the thinning of the turbulent boundary layer as Reynolds number increases.<sup>(4)</sup> At low Reynolds numbers, however, significant

dependency on Reynolds number can be expected. For instance, the thickening of the turbulent boundary layer results in a much greater displacement effect, the less energetic boundary layer may separate prematurely near the trailing edge and the laminar boundary layer may extend downstream far enough to interact with the shock wave. This more complex flow will be analysed in some detail in the following sections. The high Reynolds number behaviours of the flow will be referred to frequently to provide a complete view of the parametric variation from low to high Reynolds numbers.

Three sets of data from Reference 6 will be discussed. The first set has fixed transition at 5 percent chord with Reynolds number ranging from 4.2 to 10 million. With the high Reynolds number data from Reference 4, the forward fixing data covers a range from 4.2 to 30 million. The second and the third sets have aft transition fixings at 30 and 45 percent chord respectively with Reynolds number ranging from 4.2 to 8 million. All cases considered are at the design Mach number of 0.765.

To carry out the boundary layer manipulation procedure with aft-fixings, it is necessary to have a long extent of laminar flow over the airfoil. The results of the transition locations given in Reference 6 are replotted in Fig. 2 in terms of lift coefficient for Reynolds numbers 4.2 and 10 million. The values in between are estimated by interpolation. For a given Reynolds number and an aft-fixing location, the range of lift in which the boundary layer is fully laminar ahead of the fixing location can be determined from the figure. In the graphs for aft-fixings presented in the following sections, the lowest lift coefficient for such conditions to exist will be indicated by an arrow head. Only data at and above the indicated lift coefficient will be meaningful for the procedure

of boundary layer manipulation. Below the indicated value, transition occurs ahead of the roughness strip which then serves only to thicken the boundary layer downstream.

### 2.1 Lift, Pitching Moment and Drag

The lift versus angle of attack curves for both forward and aft-transition fixings are shown in Fig. 3a. With forward fixing, a strong Reynolds number dependency can be observed. The up-shift of the lift curve as Reynolds number increases follows directly from the reduction of the boundary layer displacement. A similar variation has been observed from the high Reynolds number data,<sup>(4)</sup> the present low Reynolds number results are, however, much more pronounced. The effect of Reynolds number diminishes as the location of the transition fixing moves downstream. This is due to the fact that the long extent of the laminar boundary layer ahead of the fixing strip has negligible displacement effect and the turbulent boundary layer aft of the strip is relatively thin because of the shorter development distance. The thinning of the turbulent boundary layer delays the trailing edge separation at high incidences and a higher maximum lift is resulted. The lift curve at Reynolds number 30 million taken from Reference 3 with free transition is also shown in each graph as a reference for comparison. This value is representative for the flight Reynolds number of a typical transport aircraft. The comparison is particularly important for validating the methodology of simulation discussed later in Section 3.

The variations of lift at a fixed angle of attack with respect to Reynolds number and the transition position are cross-plotted in Fig. 3b. The lift increases nearly linearly with Reynolds number for all three transition locations (except one data point for  $x_T/c = 0.30$  at  $Re_c = 6$

million). The high Reynolds number data taken from Reference 4 with forward fixing are also shown in the graph. The data clearly show two distinguishable trends with the dividing Reynolds number at about 10 million. It follows that an extrapolation of data from low Reynolds number to high Reynolds number will be rather complicated.

The increment of a lift for a supercritical airfoil is caused by the extension of the supercritical flow towards the rear part of the airfoil. As Reynolds number increases and the displacement effect reduces, the supercritical flow extends further downstream resulting in a net increase of lift. The extension of the low pressure region causes the negative pitching moment to increase as shown in Fig. 4a. Following the trend of the lift curve, the pitching moment curves move towards the high Reynolds number data as the transition location shifts downstream. In general, the behaviour of the pitching moment curve with forward fixing resembles closely the high Reynolds number data, although having a much lower negative value. Separation occurs at nearly the same maximum lift and as the separation moves rapidly forward the pitching moment is reduced at nearly constant lift. For aft-fixing cases, the trailing edge separation is delayed and the pitching moment is kept nearly constant towards higher lift until maximum lift is reached. Although the general level of the pitching moment approaches the high Reynolds number value as the transition position moves downstream, the behaviour of the moment curve is quite different from the latter at high lift condition. The pitching moment variation with Reynolds number at lift coefficient of 0.65 is cross-plotted in Fig. 4b. The difference in data trends below and above Reynolds number 10 million can again be observed.

The drag polars of the corresponding cases are shown in Figs.

5a. For forward fixing, the higher drag value is due to the increase of skin friction coefficient as Reynolds number decreases. As the transition position shifts downstream, the long stretch of laminar boundary layer ahead of the transition strip helps to reduce the total drag, moving the drag value towards that of the high Reynolds number. At high lift, because of the delay of the trailing edge separation, the drag rise occurs at a higher lift than that of the high Reynolds number. The cross-plot of drag against Reynolds number is shown in Fig. 5b. Again the difference of rates of variation at high and low Reynolds number ranges is clearly shown.

From the total force and moment variations, we have observed that the low Reynolds number characteristics of the airfoil is different from that at high Reynolds number. The Reynolds number dividing these two regions has a value of about 10 million. The data below this Reynolds number can only be used for extrapolation up to that value, beyond that another set of data has to be used. By moving the transition position downstream, the force and moment data tend to approach the high Reynolds number values. One has to be cautious however, that thinning of the turbulent boundary layer also changes the characteristics of the flow at high lift in a form of delaying trailing edge separation. This leads to higher value of maximum lift, lower drag and invariance of pitching moment.

## 2.2 Shock Location and Shock Mach Number

For a supercritical airfoil, the airfoil performance is mainly dictated by the extent of the supersonic flow pocket on the upper surface and the shock wave terminating it. This critical region can be examined

through two parameters, the location and the Mach number of the shock wave. The former indicates the extent of the supersonic flow and the latter the maximum expansion of the flow above the airfoil. At high lift condition, the adverse pressure gradient at the rear portion of the airfoil may cause flow separation. This process can be monitored by the trailing edge pressure and will be discussed in the next section.

The roof-top pressure distribution generated by the supercritical flow pocket is established at a lift coefficient about 0.5 and above at the design Mach number 0.765. Below this value, the supercritical flow pocket is small and the flow is mainly subcritical. This range of lift condition constitutes the linear portion of the lift versus angle of attack curve. The effect of Reynolds number appears explicitly through the boundary layer displacement in the form of decambering and will not be further discussed.

Above lift coefficient 0.5, the variations of the shock location along the upper surface of the airfoil versus lift at different Reynolds numbers and transition positions are shown in Fig. 6a. Between lift coefficient 0.6 and maximum lift, the shock is practically stationary for all cases. For forward fixing, the shock moves backward steadily as the Reynolds number increases. At high angles of attack, the trailing edge separation merges with the shock separation, and the shock moves forward rapidly as the separation propagates upstream. The reduction of the extent of the supercritical region due to flow separation is compensated by the higher expansion of the flow therein, consequently the lift drops only slightly. The behaviour of the curves in the maximum lift region is quite similar to that of the high Reynolds number which is also shown for comparison.

With aft transition fixings, the Reynolds number effect is less strong due to longer laminar flows. As the transition position shifts downstream the shock moves towards the location at high Reynolds number. Thinning of the turbulent boundary layer gives boundary properties such as momentum thickness and form factor closer to those at high Reynolds numbers, thus a better simulation for the shock-boundary layer interaction. This will be discussed further in Section 3. Because of the delay of separation due to a thin boundary layer over the rear portion of the airfoil, the shock remains at its hindmost position until separation occurs at higher lift.

The cross-plot of the shock location against Reynolds number at lift coefficient 0.65 is shown in Fig. 6b. The high Reynolds number data shown in the figure are taken from Reference 4. With forward fixing, an abrupt change of the data trend is again observed with the discontinuity located at Reynolds number 10 million, similar to that for total forces and moment as discussed in the last section. With aft-fixing, the low Reynolds number data move up as the transition location shifts backward. The rate of change with Reynolds number, however, is reduced.

The variations of shock Mach number with lift at different Reynolds numbers and transition positions are shown in Fig. 7a. The shock Mach number varies practically linearly with lift until separation occurs. After onset of separation, the shock Mach number continues to rise as the expansion around the airfoil nose steadily increases with angles of attack. With forward fixing, the shock Mach number decreases as Reynolds number increases for fixed lift. With aft-fixing, the Reynolds number effect is less pronounced. The cross-plot of the shock Mach number at

lift coefficient 0.65 against Reynolds number is shown in Fig. 7b. The variation of the data trend is similar to that of the lift coefficient shown in Fig. 3b. It is interesting to note that for a fixed angle of attack, the shock Mach number increases with Reynolds number as the decambering effect due to boundary layer displacement diminishes<sup>(4)</sup>. For fixed lift, the opposite is observed. This is due to the fact that as the decambering effect reduces, the same lift can be attained at a lower angle of attack hence lower shock Mach number.

### 2.3 Trailing Edge Pressure

Another important parameter for the flow development over the airfoil is the trailing edge pressure which indicates the condition at the rear portion of the airfoil. At low lift condition, the flow is fully attached at the trailing edge, the pressure there varies only slightly with lift as a direct result of change of boundary layer development at different lift conditions. At moderate lift until onset of separation, the trailing edge pressure is practically flat and independent of lift as shown in Fig. 8a. The behaviour of the trailing edge pressure curve is highly similar to that of the shock location shown in Fig. 6a.

With forward fixing, the trailing edge pressure at low Reynolds number is much lower than that at high Reynolds number and separation occurs at slightly lower lift than the latter. The post-stall characteristics, however, are quite similar for both low and high Reynolds numbers. As the transition location move backward, the trailing edge pressure increases and approaching that of the high Reynolds numbers. Separations, on the other hand, occur at much higher lift. The cross-plot

of the trailing edge pressure against Reynolds number at lift coefficient 0.65 is shown in Fig. 8b. Again the low and high Reynolds numbers trends can be observed. With aft-fixing, the value approaches quite close to that of high Reynolds number in contrast to the shock location which is always below the high Reynolds number value. It should be noted that the shock-boundary layer interaction depends on the boundary layer development ahead of the shock while the flow over the trailing edge region develops from the boundary layer after the interaction. Since the interaction works like an amplifier for the boundary layer upstream of the shock,<sup>(7)</sup> a small difference ahead of the shock will be exaggerated after the interaction and leads to a gross difference in development of the trailing edge flow.

#### 2.4 General Characteristics of Low Reynolds Number Flows

In the preceding section, we have examined the data for the low Reynolds numbers at both forward and aft-fixings and compared them with the high Reynolds number data. The analysis shows a distinct data trend with higher sensitivity to Reynolds number variation for the low Reynolds number data. The dividing value of these two trends is about 10 million. As the transition position moves backward, the value of the low Reynolds number data approach those at high Reynolds number. Thinning of the boundary layer due to aft-fixing, however, delays the trailing edge separation and yields much higher maximum lift. With this information, the implication of simulation of high Reynolds number flow using low Reynolds number data will be investigated in the next section.

#### 3. Simulation and Extrapolation

With both the low and high Reynolds number data available, we are now in a position to investigate in what range of Reynolds number that

simulation can be applied to and the feasibility of extrapolating the data to a higher Reynolds number. The data trend with respect to Reynolds number is first examined and then the direct simulation is discussed. Finally the simulation and extrapolation scenarios given in Reference 8 on the simulation methodology applicable to the present data are identified.

With forward fixing, the data show clearly two distinct trends for low and high Reynolds numbers with the dividing value at about 10 million. This dividing Reynolds number is defined as the critical Reynolds number in the simulation/extrapolation methodology.<sup>(8)</sup> The parameter is critical in that there is a change of simulation trend which affects critically the extrapolation process from low to high Reynolds numbers. The critical Reynolds number is clearly revealed if Reynolds number sweep is performed as in the present study. However, it is not possible to identify it if only low Reynolds number data are available.<sup>(8)</sup> This will be discussed further later in this section.

The aft-fixing data show the range of Reynolds numbers that direct simulation can be applied. Simulation implies that by manipulating the boundary layer by tripping at the mid or rear position at the test Reynolds number, the aerodynamic parameters so generated are the same as those at a higher Reynolds number with a forward transition position corresponding to that which may occur in flight. The simulated Reynolds number is defined as effective Reynolds number.<sup>(8)</sup> All aerodynamic parameters analysed in Section 2 can be chosen as a simulation criterion. The total force and moment data, however, give only global results and lack details of the flow. Thus the shock location or the shock Mach number relating directly to the flow development over the airfoil are the obvious choice.

Simulation of shock location can be carried out as follows. For a given data point with aft-fixing at low Reynolds number, the simulated Reynolds number or the effective Reynolds number can be read from the forward fixing curve having the same shock location (Fig. 6b). The present results show for this particular airfoil, that all simulations are limited to Reynolds number below the critical Reynolds number. A similar observation can be made if the shock Mach number is used as the simulation criterion. A direct simulation to conditions above the critical Reynolds number do not seem to be achievable, in contrast to Reference 7 which shows that the flow at Reynolds number 30 million can be simulated with 45 percent fixing at Reynolds number 2.4 million. Since the maximum effective Reynolds number is always smaller than the critical Reynolds number, the simulation scenario will be in the category 4 ( $R_{\text{flight}} > R_{\text{crit}} > \max R_{\text{eff}}$ ) and 5 ( $R_{\text{crit}} > R_{\text{flight}} > \max R_{\text{eff}}$ ) given in Reference 8. A variation of scenario 2 ( $R_{\text{crit}} > \max R_{\text{eff}} > R_{\text{flight}}$ ) can also be treated as a direct simulation. Both cases 4 and 5 require extrapolation, a direct extrapolation for case 5 and two steps (from  $R_{\text{eff}}$  to  $R_{\text{crit}}$  to  $R_{\text{flight}}$ ) for case 4.

The simulation criterion plot shown here is constructed from experimental data which cover a wide range of Reynolds number. This complete overview of the variation of the aerodynamic parameter is not always available if tests are performed in a tunnel of low Reynolds number capacity. The trend of variation of the aerodynamic parameter has then to be evaluated by computation and the value of critical Reynolds number estimated by comparison of measured and predicted trends.<sup>(8)</sup> This approach has also been examined in the present study. The computational results obtained from the transonic airfoil code GRUMFOIL<sup>(9)</sup> are shown in

Fig. 9. Although this code is designed for airfoils with cusped trailing edges, it is adopted for the present airfoil with a slight trailing edge bluntness of 0.5% chord. The shock locations are well predicted above the critical Reynolds number but much over predicted below the critical value. The discrepancy is aggravated further as the transition position moves downstream. The failure of computation may be attributed to the inadequacy of the code in modelling the strong viscous-inviscid interaction at low Reynolds numbers. Allowing for trailing edge separation by using the inverse boundary layer method does improve the prediction of the shock location but separations are predicted at about 80 percent chord for all cases. No separation was observed at these conditions in the experiment however. Without a reliable code for the low Reynolds number range, a simulation criterion plot cannot be constructed and the computational approach can not be pursued any further in the present exercise. It should be noted, however, that the computation for high Reynolds number is accurate and can be adequately used for extrapolation from the critical Reynolds number to a higher value.

For simulation at higher lift condition, it is necessary to reverse the transition location back toward the leading edge. At these conditions, the thin boundary layer generated by aft-fixing fails to separate, yielding a maximum lift much higher than that at high Reynolds numbers. Forward fixing, however, shows a much closer simulation as discussed in Section 2.

#### 4. Conclusion

The low Reynolds number data from 4.2 to 10 million at the design Mach number 0.765 for the CAST 10-2/DOA 2 airfoil have been analysed for its Reynolds number effects. The data with forward transition fixing have been examined in association with the high Reynolds number data obtained in previous tests to reveal the variation of its Reynolds number dependency. The data with aft-fixing have been investigated in the light of boundary layer manipulation for simulating high Reynolds number flows. The observations made are summarized as follows:

1. With forward transition fixing, the trend for the low Reynolds number data differs from that of high Reynolds number data. The trend is much more sensitive to Reynolds number variation and is attributed to the strong viscous-inviscid flow interaction at low Reynolds numbers.
2. The Reynolds number dividing these two trends for low and high Reynolds numbers has a value about 10 million.
3. With transition fixing moving downstream, the low Reynolds number data approach those at high Reynolds numbers.
4. Thinning of the boundary layer with aft-fixing delays the trailing edge separation and generates much higher maximum lift.
5. With respect to simulation of high Reynolds number flow, the discontinuity of Reynolds number trend makes the extrapolation of the simulation parameter from low to high Reynolds numbers a two-step process. It is essential that the critical Reynolds number dividing these two trends is well determined.
6. At the cruise condition, simulation of higher Reynolds number flows can be achieved by aft-fixings. However, the effective Reynolds

number simulated is still below the critical Reynolds number for the airfoil model. A direct simulation of high Reynolds flow beyond the critical value has not been accomplished.

7. At high lift condition, transition fixing should move forward for better simulation of the trailing edge flow.
8. The present results substantiate the principle of the simulation and extrapolation methodology proposed by the AGARD/FDP<sup>(1,8)</sup>.
9. The computational code presently available has limited capability in predicting low Reynolds number flows. Extensive applications of computational methods for the estimation of Reynolds number effects as proposed by the Methodology cannot be carried out for the present case.

The present study has demonstrated two distinct characteristics of Reynolds number effects at low and high values respectively. It has also determined the positions of transition fixing for simulating higher Reynolds number flow at different lift conditions. Although it has not been able to follow the AGARD methodology procedure with full applications of computational methods, it has explicitly substantiated the basic principle of the methodology by revealing the Reynolds number effects over a wide range of Reynolds numbers. The data analyses presented can readily be used for a similar exercise on the Methodology in the future when more advanced computational codes are available.

References

1. Laster, H.L. Ed. Boundary Layer Simulation and Control in Wind Tunnels. AGARD Advisory Report No. 224, April 1988.
2. Chan, Y.Y. Wind Tunnel Investigation of CAST 10-2/DOA 2 12% Supercritical Airfoil Model. LTR-HA-5×5/0162, National Aeronautical Establishment, National Research Council Canada, May 1986.
3. Chan, Y.Y. Wind Tunnel Investigation of CAST 10-2/DOA 2 12% Supercritical Airfoil Model, Phase II, LTR-HA-5×5/0170, National Aeronautical Establishment, National Research Council Canada, June 1987.
4. Chan, Y.Y. Analysis of Experimental Data for CAST 10-2/DOA 2 Supercritical Airfoil at High Reynolds Numbers. NAE-AN-49, National Aeronautical Establishment, National Research Council Canada, January, 1988.
5. Stanewsky, E. High Reynolds Number Tests of the Demurie, F. CAST 10-2/DOA 2 Transonic Airfoil at Ambient Ray, E.J. and Cryogenic Temperature Conditions. AGARD Johnson, C.B. CP-348, Wind Tunnels and Testing Techniques. September 1983.

6. Chan, Y.Y. Wind Tunnel Investigation of CAST 10-2/DOA 2  
12% Supercritical Airfoil Model, AGARD  
Methodology. LTR-HA-5×5/0181, National  
Aeronautical Establishment, National Research  
Council Canada, October, 1988.

7. Stanewsky, E. Interaction Between the Outer Inviscid Flow  
and the Boundary layer on Transonic Airfoil.  
Z. Flugwiss. Weltraumforsch. 7(1983), Heft 4,  
pp. 242-252.

8. Haines, A.B. An Outline of the Methodology, Section 3.2.1.  
Elsenaar, A. in Section 3, Simulation/Extrapolation  
Methodology, Boundary Layer Simulation and  
Control in Wind Tunnel, AGARD Advisory Rept.  
No. 224, April, 1988.

9. Mead, H.R. GRUMFOIL: A Computer Code for the Viscous  
Melnik, R.E. Transonic Flow Over Airfoils. NASA Contractor  
Report 3806. October 1985.

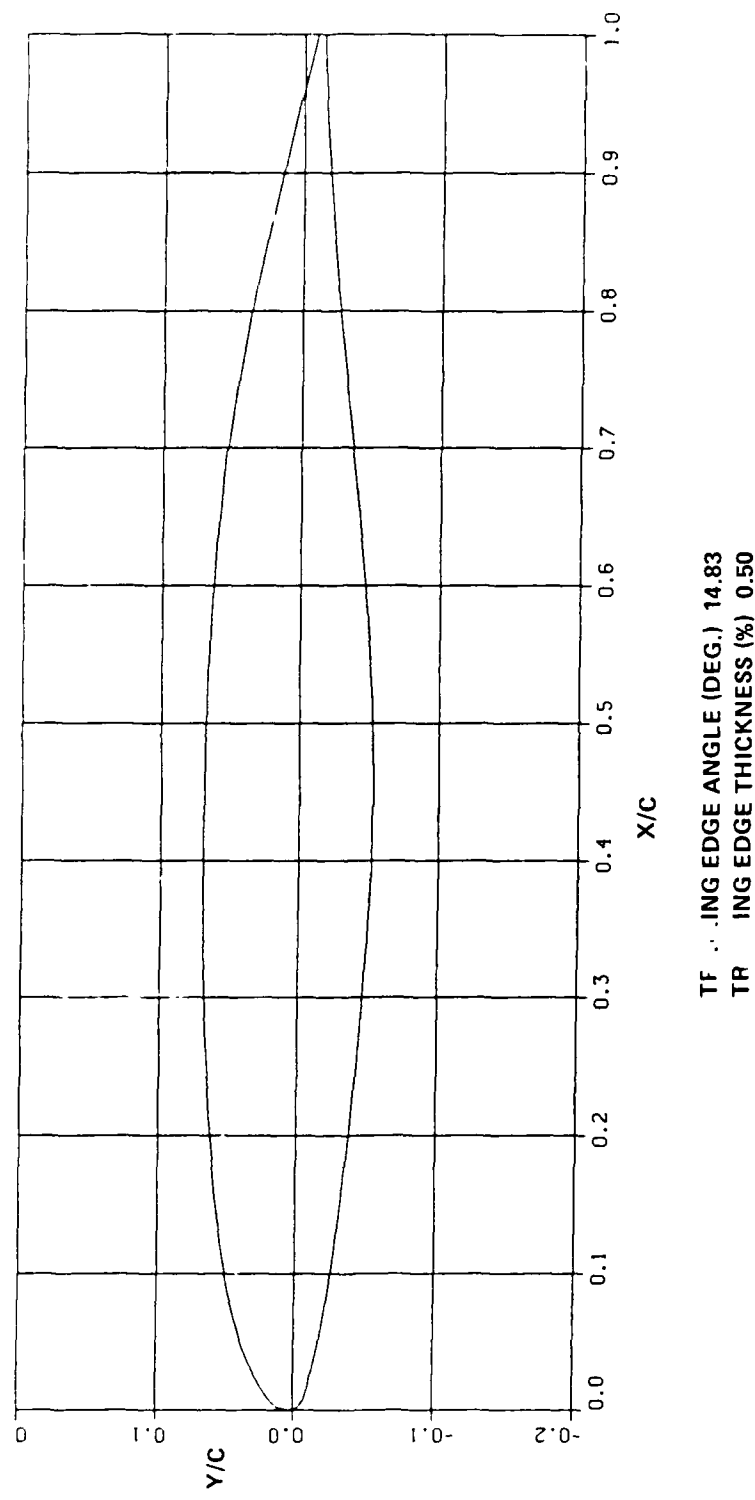


FIG. 1: SECTION PROFILE OF CAST 10-2/DOA2 AIRFOIL

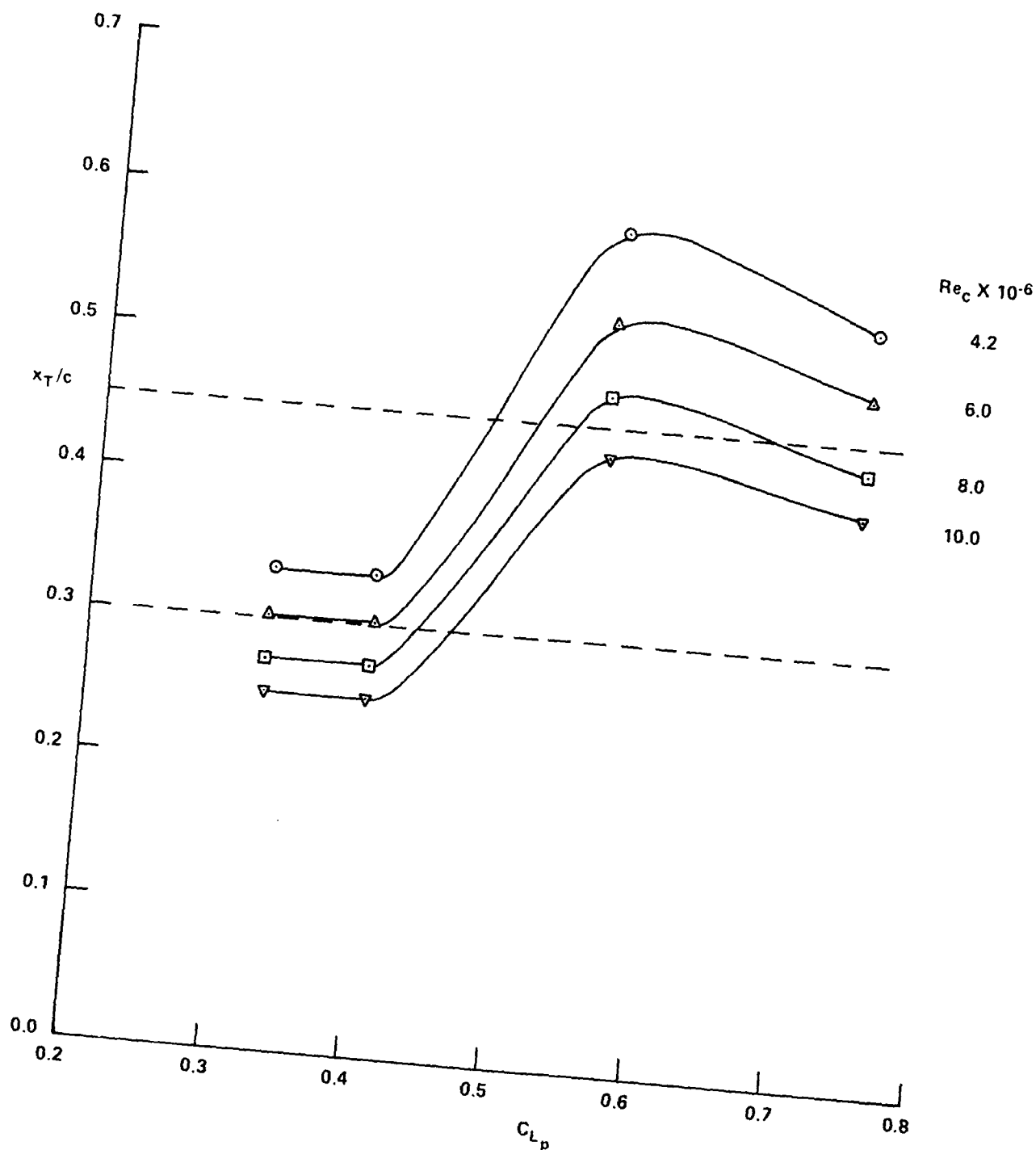


FIG. 2: ESTIMATIONS OF NATURAL TRANSITION LOCATIONS AT THE  
UPPER SURFACE OF THE AIRFOIL,  $M_\infty = 0.765$

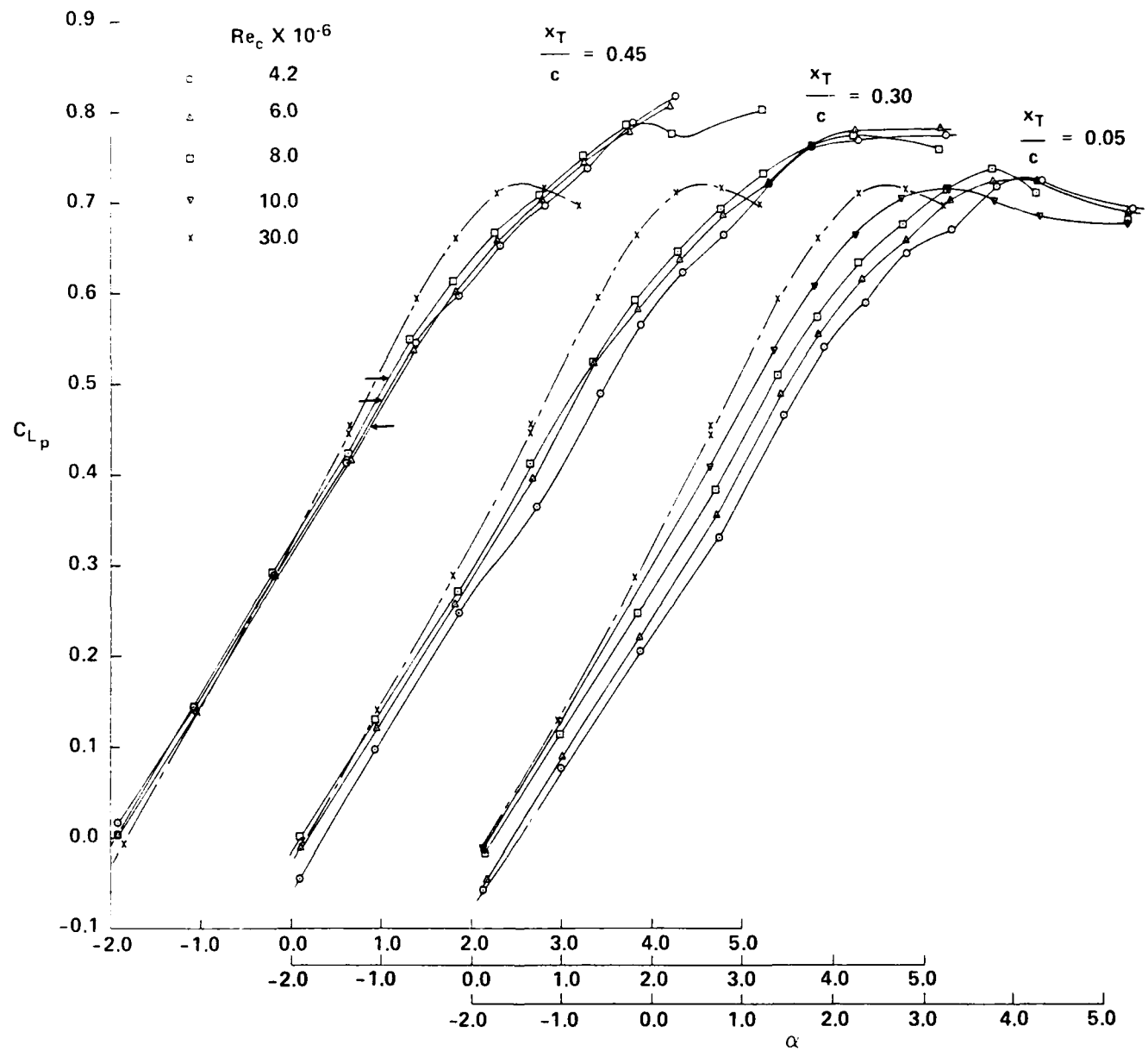


FIG. 3(a): LIFT VERSUS ANGLES OF ATTACK AT VARIOUS REYNOLDS NUMBERS WITH FORWARD AND AFT TRANSITION FIXINGS,  
 $M_\infty = 0.765$

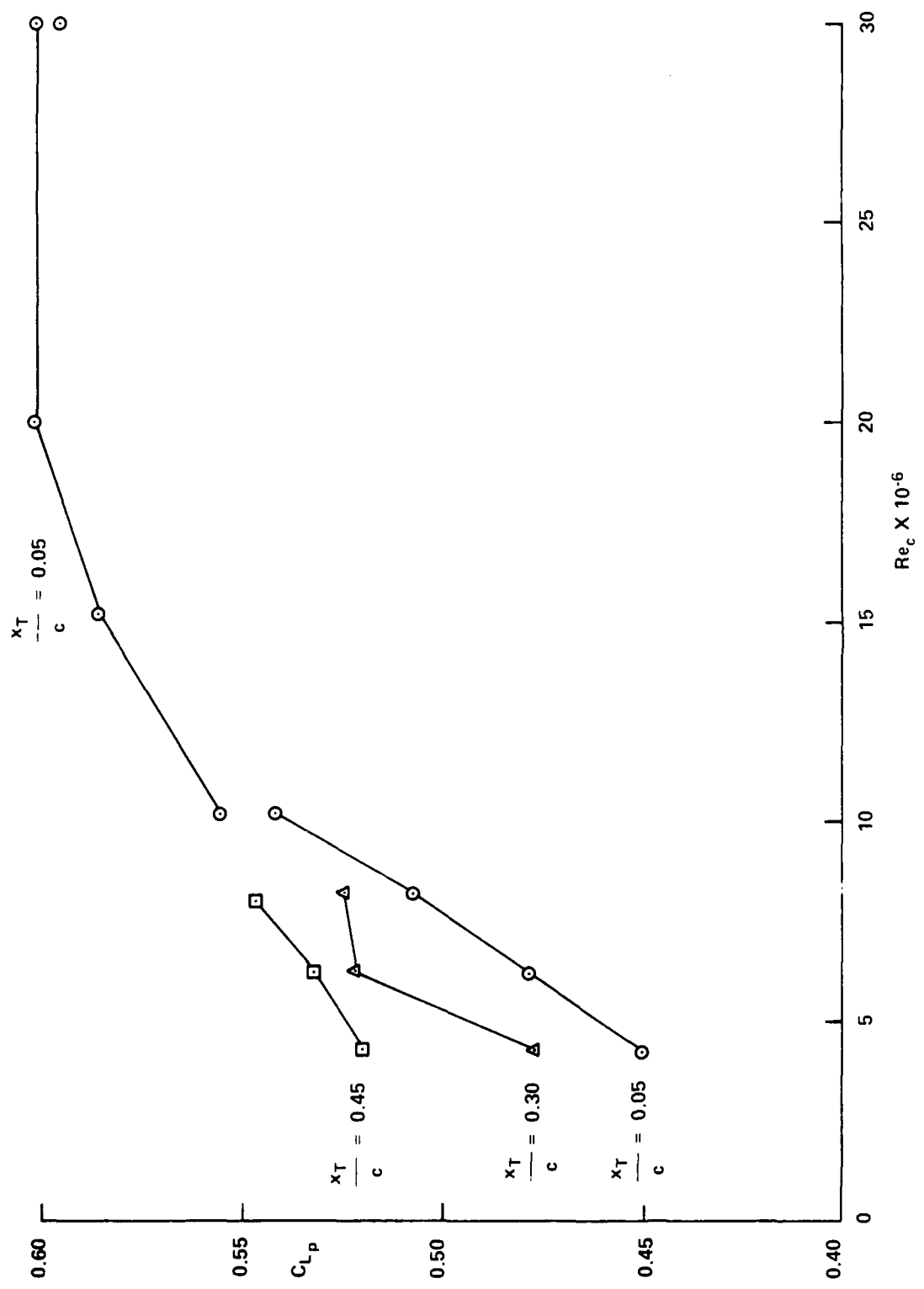


FIG. 3(b): REYNOLDS NUMBER DEPENDENCE OF LIFT AT AN ANGLE  
OF ATTACK  $\alpha = 1.35$  degrees,  $M_\infty = 0.765$

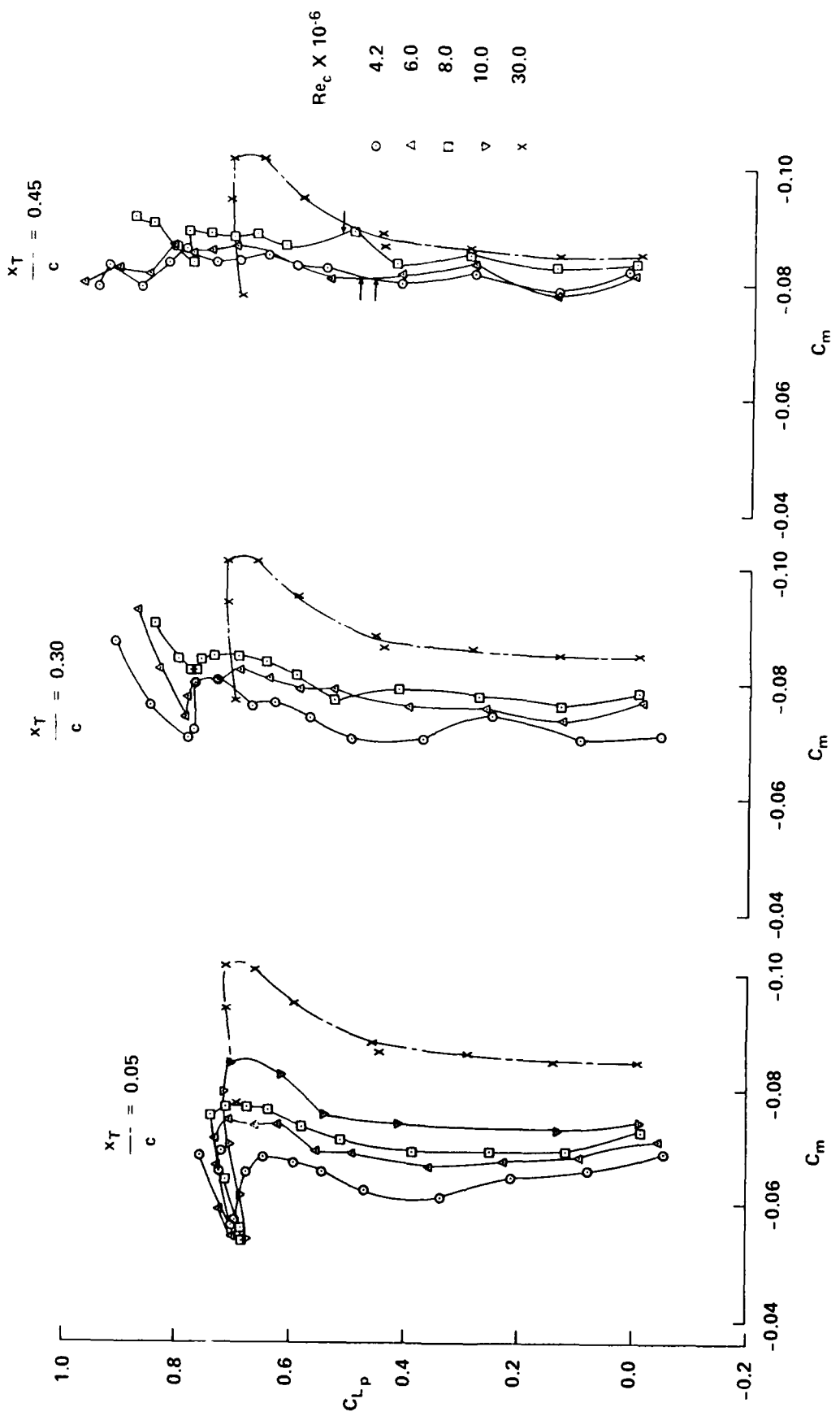


FIG. 4(a): PITCHING MOMENT VERSUS LIFT AT VARIOUS REYNOLDS NUMBERS WITH FORWARD AND AFT TRANSITION FIXINGS,  
 $M_\infty = 0.765$

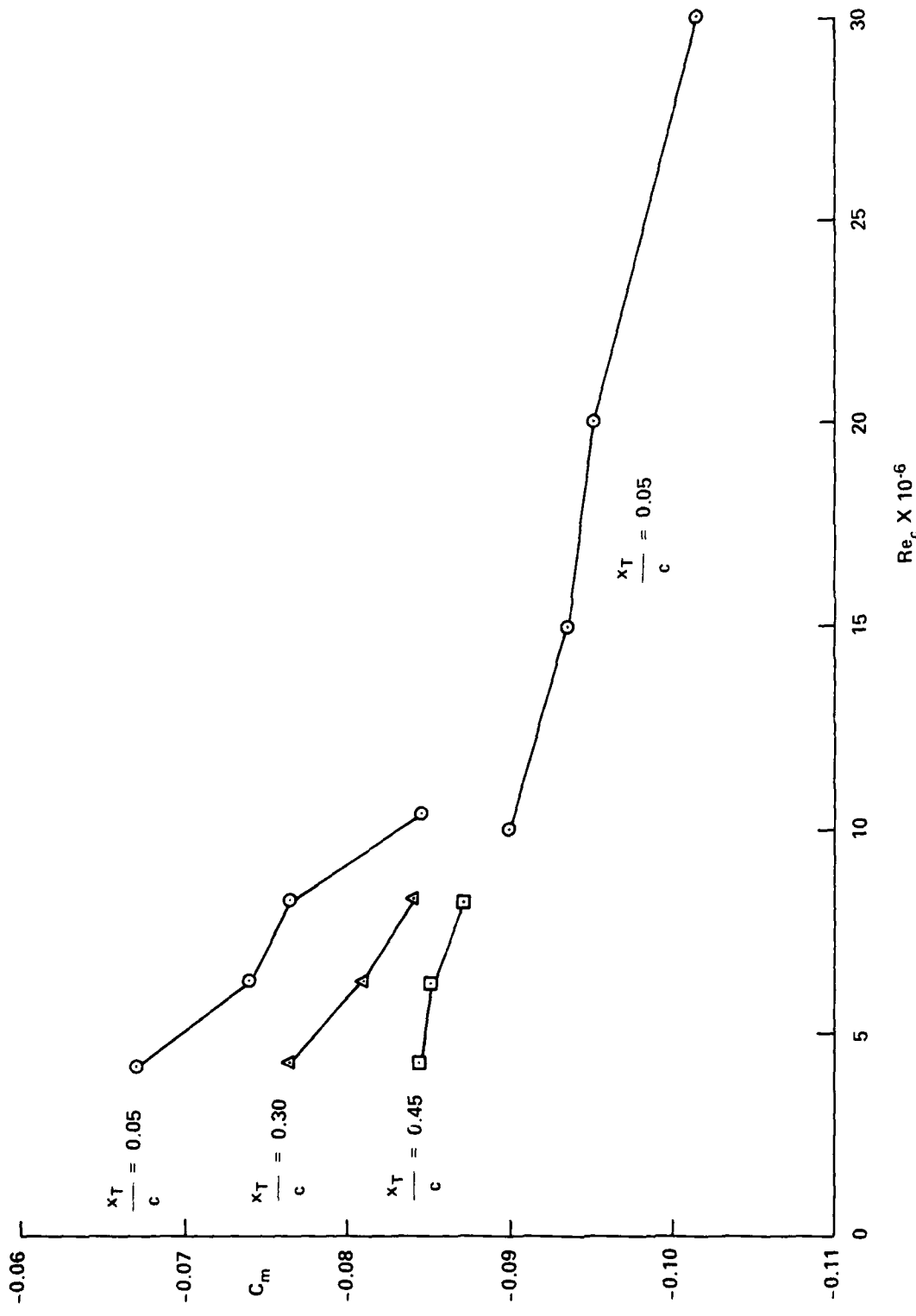


FIG. 4(b): REYNOLDS NUMBER DEPENDENCE OF PITCHING MOMENT  
AT CONSTANT LIFT  $C_{Lp} = 0.65$ ,  $M_\infty = 0.765$

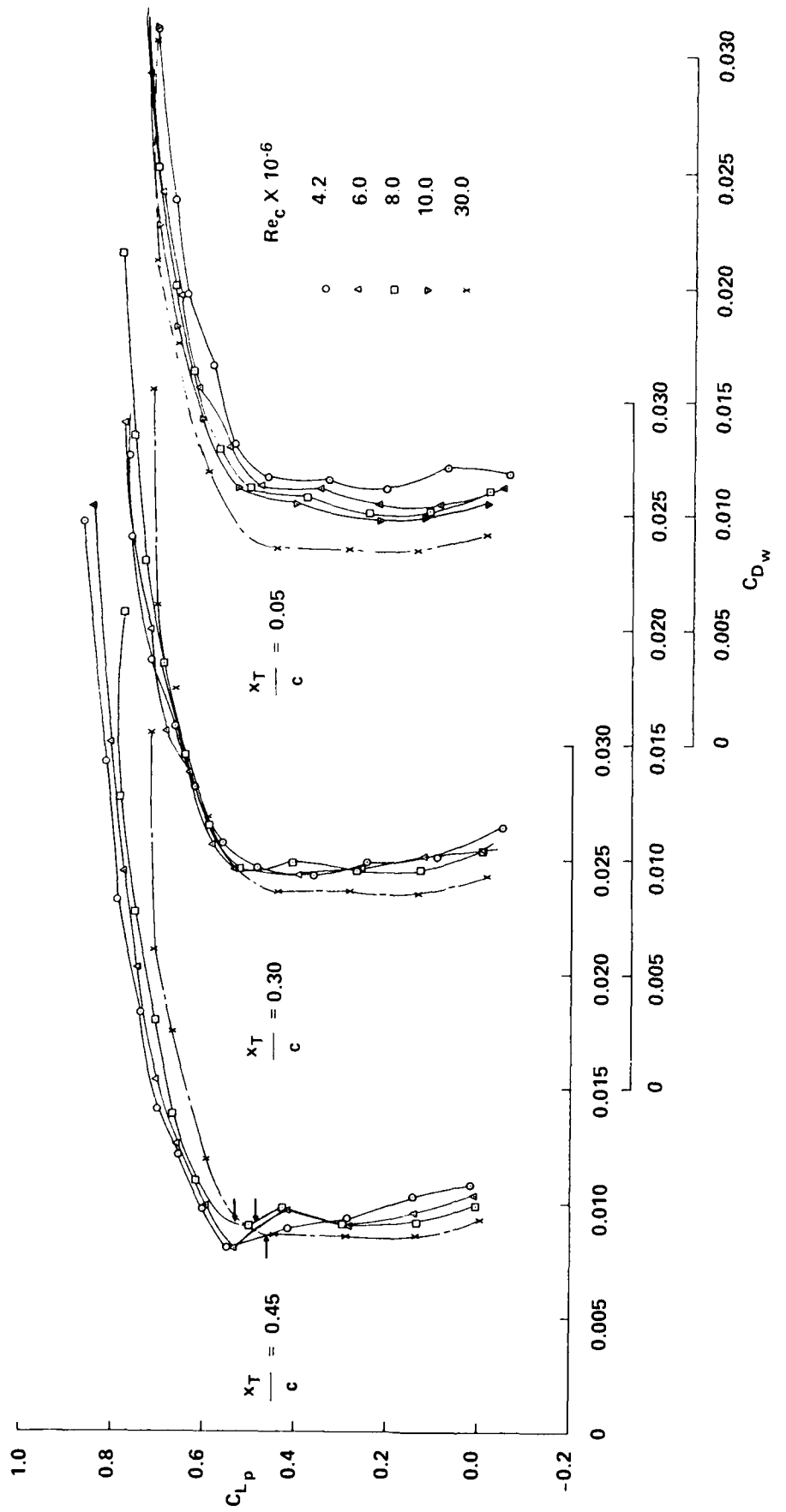
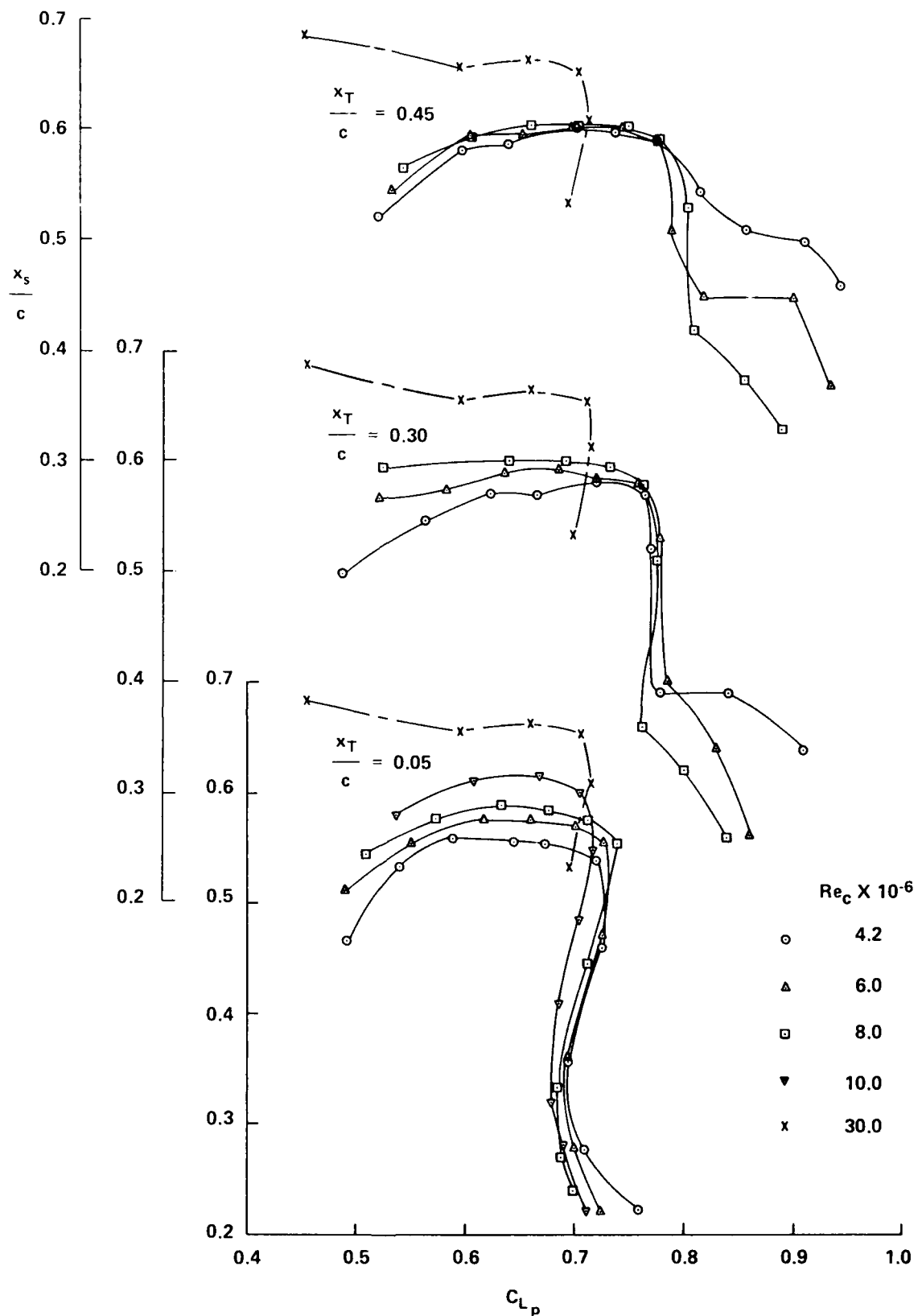


FIG. 5(a): DRAG VERSUS LIFT AT VARIOUS REYNOLDS NUMBERS  
WITH FORWARD AND AFT TRANSITION FIXINGS,  
 $M_\infty = 0.765$



**FIG. 6(a): SHOCK LOCATION VERSUS LIFT AT VARIOUS REYNOLDS NUMBER WITH FORWARD AND AFT TRANSITION FIXINGS,  $M_\infty = 0.765$**

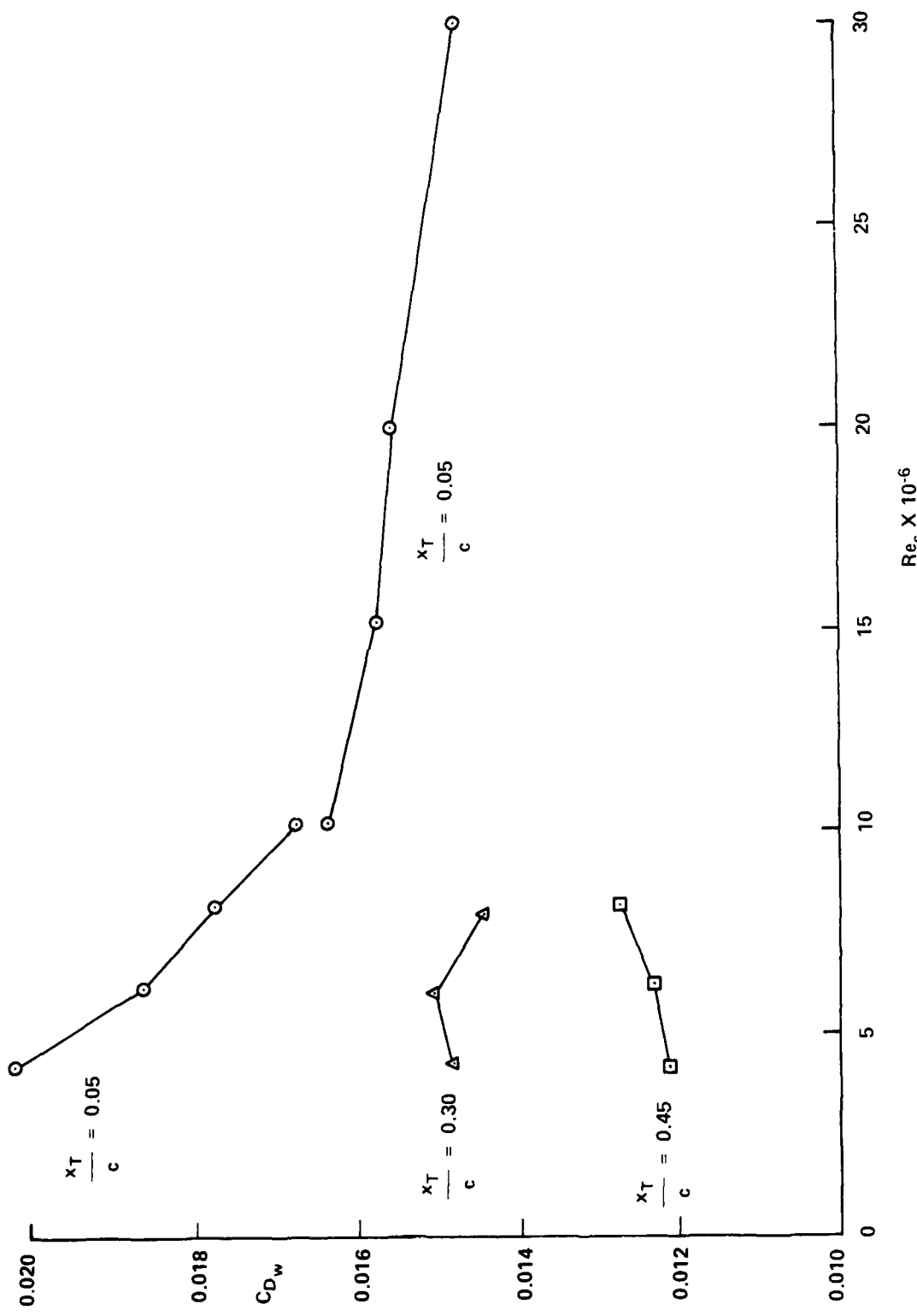
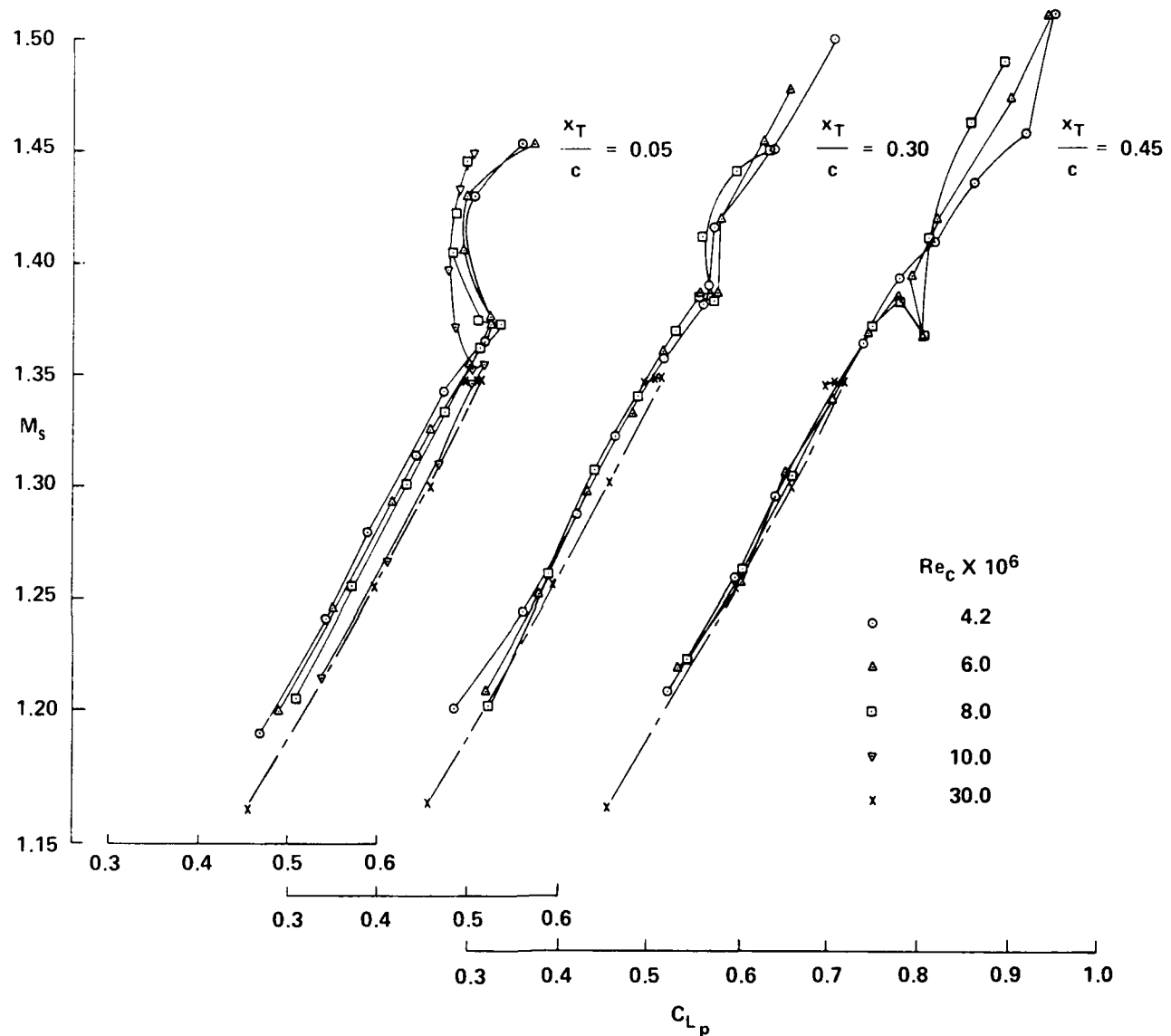


FIG. 5(b): REYNOLDS NUMBER DEPENDENCE OF DRAG AT  
CONSTANT LIFT,  $C_{L_p} = 0.65, M_\infty = 0.765$



**FIG. 7(a): SHOCK MACH NUMBER VERSUS LIFT AT VARIOUS REYNOLDS NUMBERS WITH FORWARD AND AFT TRANSITION FIXINGS,  $M_\infty = 0.765$**

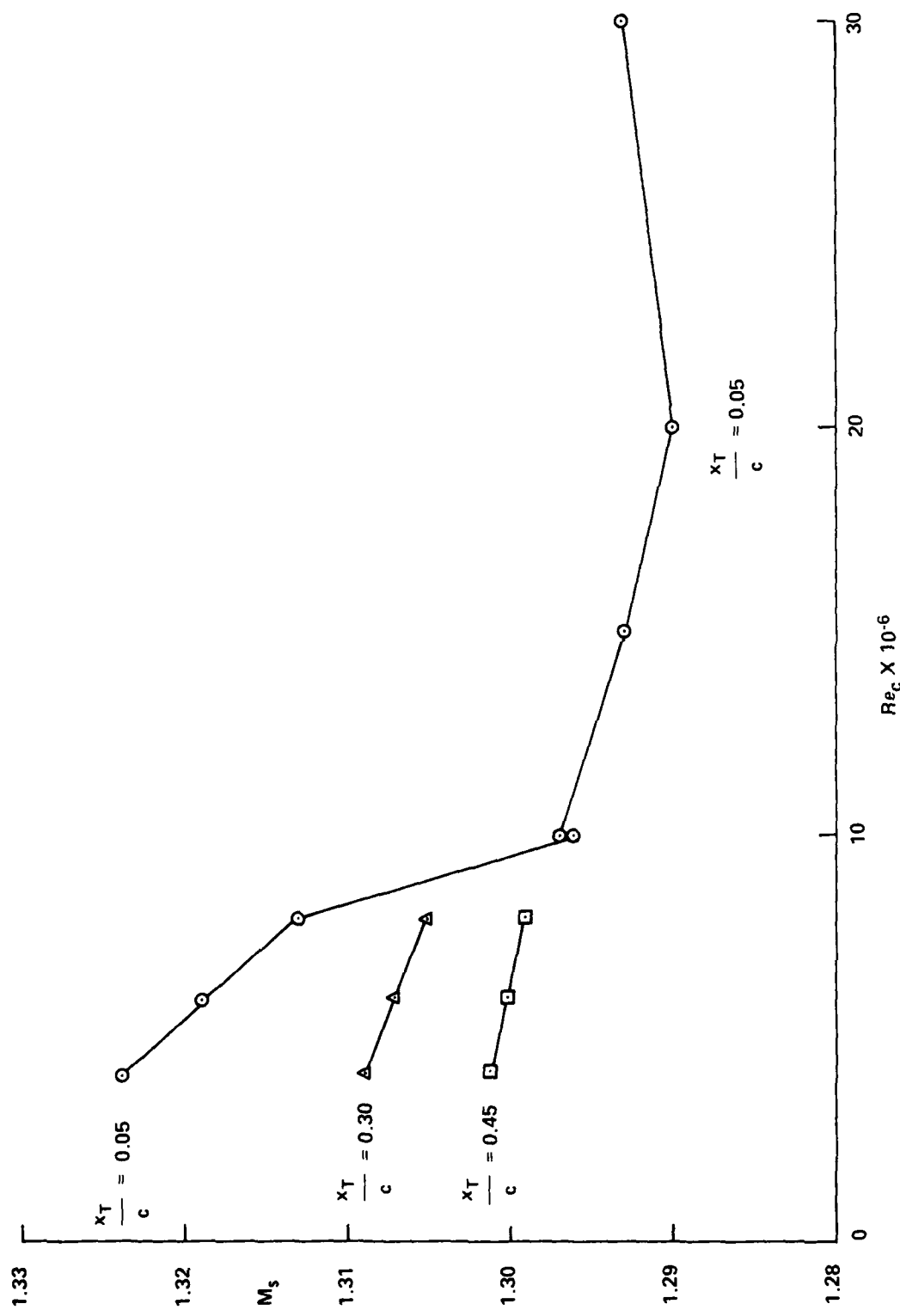


FIG. 7(b): REYNOLDS NUMBER DEPENDENCE OF SHOCK MACH NUMBER AT CONSTANT LIFT,  $C_{Lp} = 0.65$ ,  $M_\infty = 0.765$

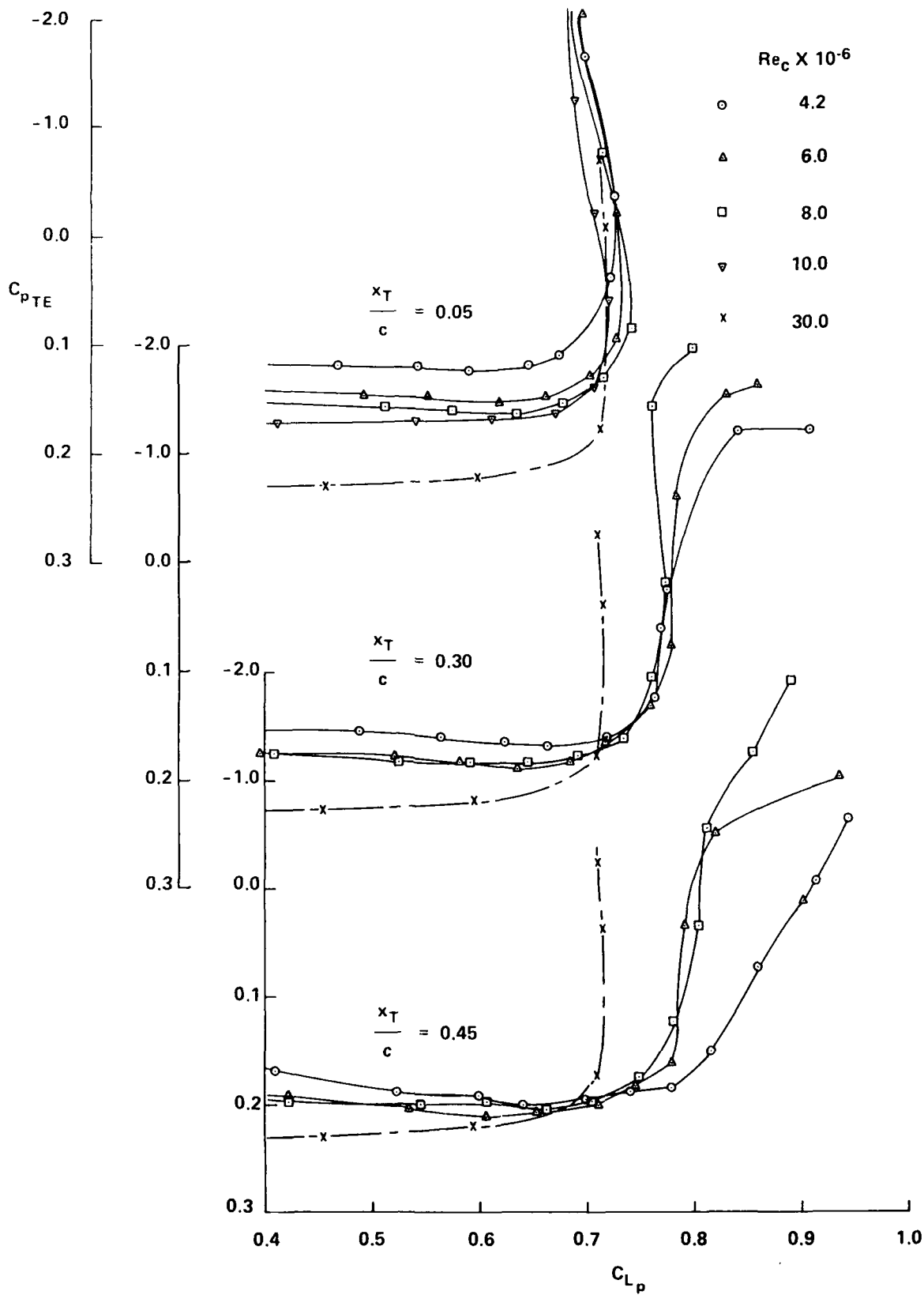


FIG. 8(a): TRAILING EDGE PRESSURE VERSUS LIFT AT VARIOUS REYNOLDS NUMBERS WITH FORWARD AND AFT TRANSITION FIXINGS,  $M_\infty = 0.765$

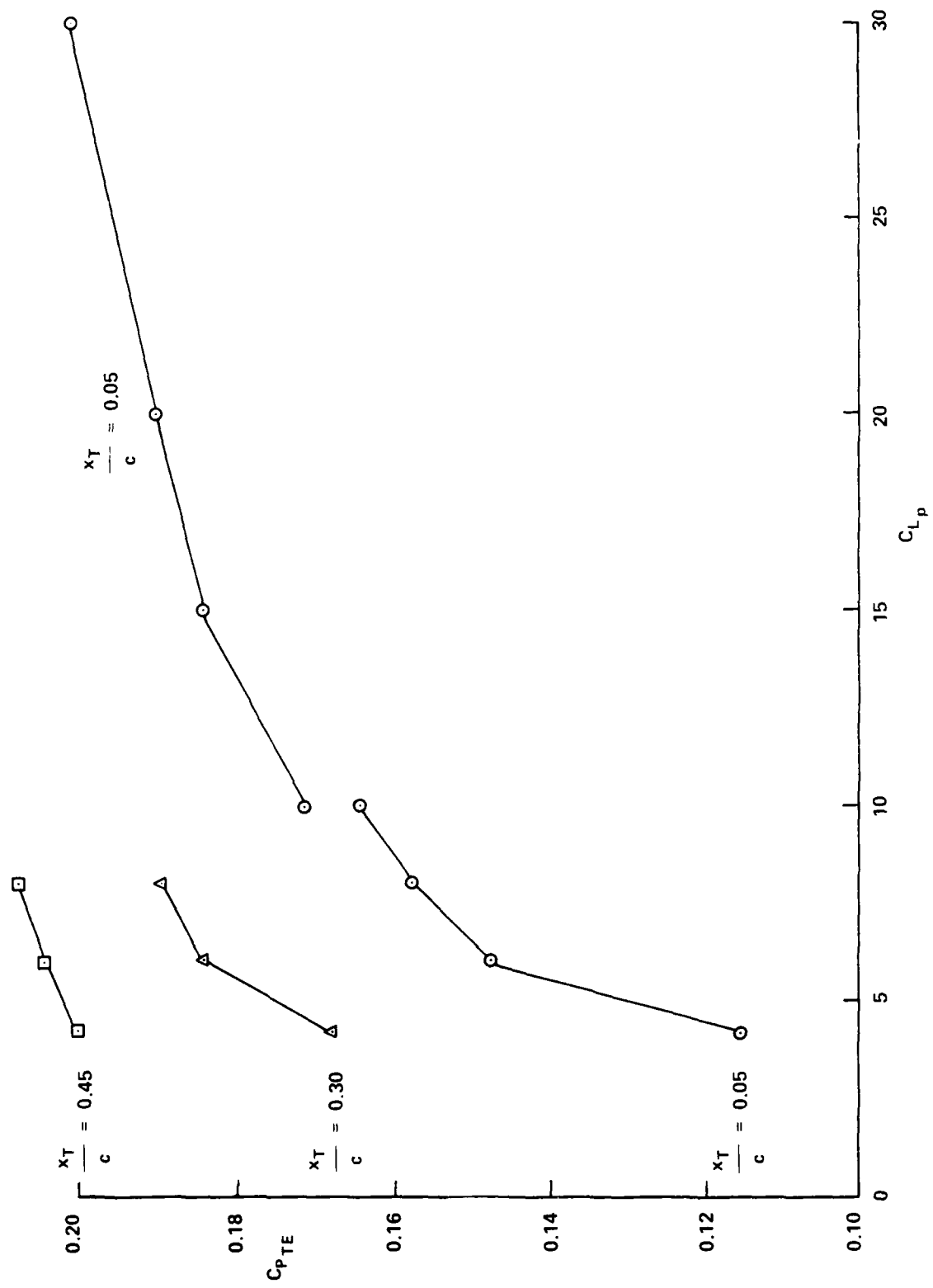


FIG. 8(b): REYNOLDS NUMBER DEPENDENCE OF TRAILING EDGE PRESSURE AT CONSTANT LIFT,  
 $C_{L_p} = 0.65$ ,  $M_\infty = 0.765$

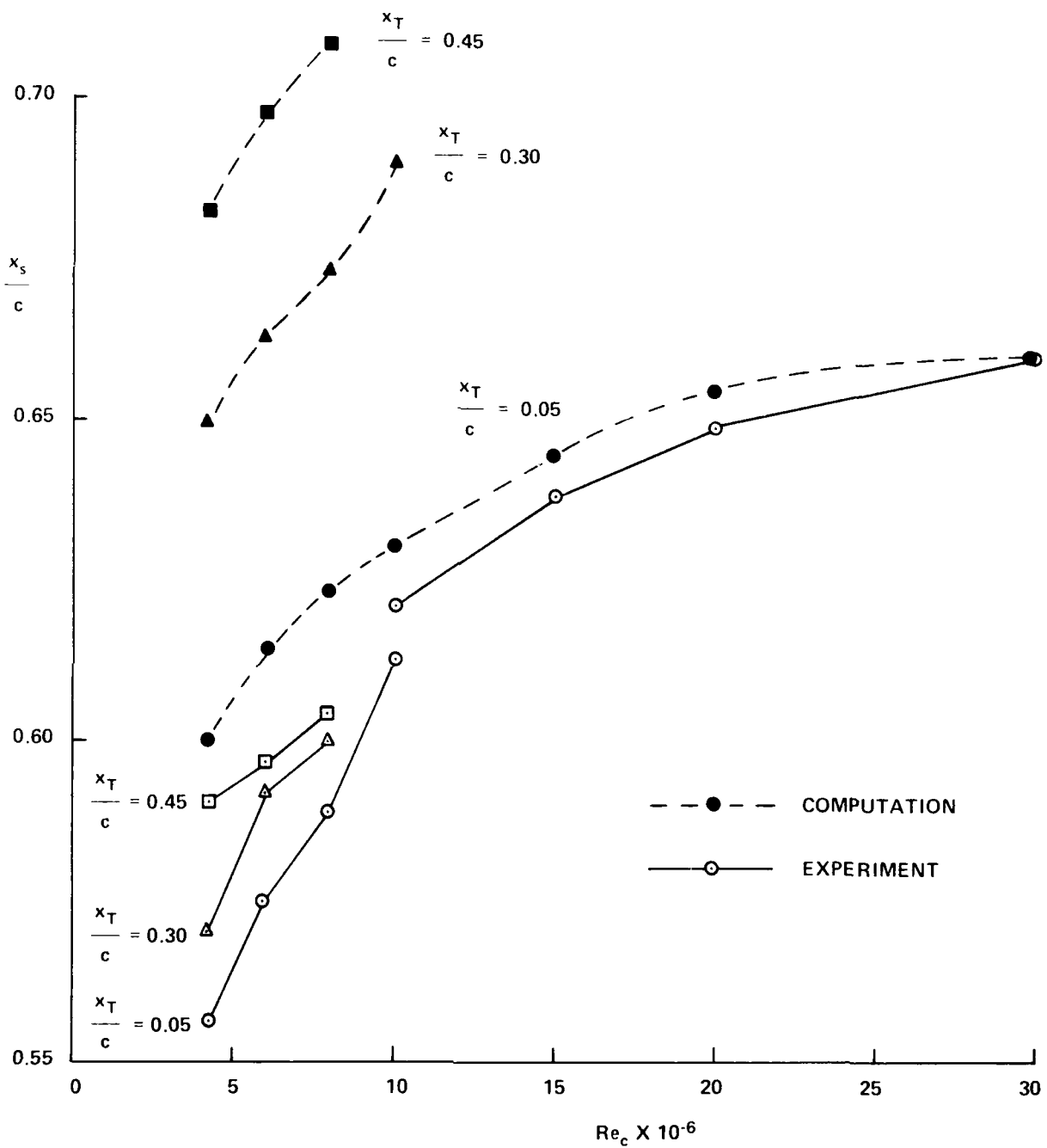


FIG. 9: COMPUTATIONAL RESULTS FOR THE SIMULATION CRITERION IN COMPARISON WITH EXPERIMENTAL DATA  
 $C_{L_p} = 0.65, M_\infty = 0.765$

**REPORT DOCUMENTATION PAGE / PAGE DE DOCUMENTATION DE RAPPORT**

REPORT/RAPPORT NAE-AN-60		REPORT/RAPPORT NRC No. 30268	
1a		1b	
REPORT SECURITY CLASSIFICATION CLASSIFICATION DE SÉCURITÉ DE RAPPORT		DISTRIBUTION (LIMITATIONS)	
2 Unclassified		3 Unlimited	
TITLE/SUBTITLE/TITRE/SOUS-TITRE Analysis of Experimental Data for CAST 10-2/DOA 2 Supercritical Airfoil at Low Reynolds 4 Numbers and Application to High Reynolds Number Flow			
AUTHOR(S)/AUTEUR(S) 5 Y.Y. Chan			
SERIES/SÉRIE 6 Aeronautical Note			
CORPORATE AUTHOR/PERFORMING AGENCY/AUTEUR D'ENTREPRISE/AGENCE D'EXÉCUTION 7 National Research Council Canada National Aeronautical Establishment High Speed Aerodynamics Laboratory			
SPONSORING AGENCY/AGENCE DE SUBVENTION 8			
DATE 9 89-01	FILE/DOSSIER 10	LAB. ORDER COMMANDÉ DU LAB. 11	PAGES 40 12a
FIGS/DIAGRAMMES 9 12b			
NOTES 13			
DESCRIPTORS (KEY WORDS)/MOTS-CLÉS 14 1. Airfoils — supercritical 2. Transonic 3. Reynolds numbers			
SUMMARY/SOMMAIRE 15			
<p>The experimental investigation of CAST 10-2/DOA 2 supercritical airfoil previously conducted in the NAE Two-Dimensional Test Facility has been extended to low Reynolds number range at the design Mach number 0.765. The results indicate that with forward transition fixing, the data trend at low Reynolds number is different from that at high Reynolds number with the former more sensitive to the Reynolds number variation. The dividing Reynolds number for these two regions is about 10 million. With aft fixing, the low Reynolds number data approach those at higher Reynolds numbers for cruise conditions. However, at high lift conditions the thin boundary layer delays separation and higher maximum lift is obtained. The characteristics of the Reynolds number dependency obtained from the analysis substantiate the principle of the simulation/extrapolation methodology for data obtained from low Reynolds number to flight Reynolds number as proposed by the AGARD/Fluid Dynamics Panel.</p>			